

# Developing Analysis, Modeling, and Simulation Tools for Connected Automated Vehicle Applications: A Case Study on SR 99 in California

PUBLICATION NO. FHWA-HRT-21-039

MARCH 2021



U.S. Department of Transportation  
**Federal Highway Administration**

Research, Development, and Technology  
Turner-Fairbank Highway Research Center  
6300 Georgetown Pike  
McLean, VA 22101-2296

## FOREWORD

Connected automated vehicle (CAV) technology is expected to produce significant mobility, safety, and environmental benefits for the traveling public. However, real-world case studies are needed to articulate reasonable benefits attributable to the technology. This report details a case study on the impact of vehicle connectivity and automated longitudinal control (i.e., SAE J3016 driving automation Level 1) on SR 99 in California to explore the benefits of cooperative adaptive cruise control on mobility and environmental performance measures.<sup>(1)</sup> This report may be of interest to State and local departments of transportation looking to better understanding possible real-world impacts of CAV technology.

Brian P. Cronin, P.E.  
Director of Safety and Operations  
Research and Development

### Notice

This document is disseminated under the sponsorship of the U.S. Department of Transportation (USDOT) in the interest of information exchange. The U.S. Government assumes no liability for the use of the information contained in this document.

The U.S. Government does not endorse products or manufacturers. Trademarks or manufacturers' names appear in this report only because they are considered essential to the objective of the document.

### Quality Assurance Statement

The Federal Highway Administration (FHWA) provides high-quality information to serve Government, industry, and the public in a manner that promotes public understanding. Standards and policies are used to ensure and maximize the quality, objectivity, utility, and integrity of its information. FHWA periodically reviews quality issues and adjusts its programs and processes to ensure continuous quality improvement.

## TECHNICAL REPORT DOCUMENTATION PAGE

1. Report No. FHWA-HRT-21-039	2. Government Accession No.	3. Recipient's Catalog No.	
4. Title and Subtitle Developing Analysis, Modeling, and Simulation Tools for Connected Automated Vehicle Applications: A Case Study on SR 99 in California		5. Report Date March 2021	
		6. Performing Organization Code	
7. Author(s) Hao Liu (ORCID: 0000-0001-5585-6576), Xiao-Yun Lu (ORCID: 0000-0001-6491-3990), Steven E. Shladover (ORCID: 0000-0002-3207-0084), and Zhitong Huang (ORCID: 0000-0003-2871-6302)		8. Performing Organization Report No.	
9. Performing Organization Name and Address Leidos, Inc. 11251 Roger Bacon Drive Reston, VA 20190  California PATH Program, Institute of Transportation Studies University of California, Berkeley Richmond Field Station 1357 S. 46th Street Richmond, CA 94804		10. Work Unit No.	
		11. Contract or Grant No. DTFH6116D00030, Task Order 22	
12. Sponsoring Agency Name and Address U.S. Department of Transportation Federal Highway Administration 1200 New Jersey Avenue, SE Washington, DC 20590		13. Type of Report and Period Covered Final Report; September 2020	
		14. Sponsoring Agency Code HRDO-20	
15. Supplementary Notes The government Task Managers were John Halkias (HOTM-1), who led application development, and Gene McHale (HRDO-20; ORCID: 0000-0003-1031-6538), who led the case study.			
16. Abstract The purpose of this report is to document a simulation-based case study investigating the effectiveness of SAE J3016 Level 1 automation technology for mitigating or solving existing transportation problems related to congestion, fuel consumption, and emissions. <sup>(1)</sup> This case study examined the impacts of cooperative adaptive cruise control (CACC) vehicle string operations on traffic performance and fuel consumption on the 13-mi SR 99 northbound corridor from Elk Grove Boulevard to SR 50 near Sacramento. The research team evaluated the performance of the busy urban corridor under various CACC market penetration scenarios, traffic demand inputs, and CACC management strategies. Specifically, the research team examined average vehicle speed, average vehicle miles traveled per gallon of fuel consumed, average string length, and CACC vehicle string probability (i.e., the probability of a CACC vehicle operating in a string) at CACC market penetration rates of 0, 20, 40, 60, 80, and 100 percent. The study investigated the corridor's spatiotemporal traffic patterns under the existing traffic demand and with the demand increased by 20 percent. Additionally, it analyzed CACC string operation after vehicle awareness device and CACC managed lane strategies were implemented.			
17. Key Words Connected automated vehicle, cooperative adaptive cruise control, microscopic traffic modeling, CACC vehicle string operation, vehicle fuel consumption		18. Distribution Statement No restrictions. This document is available to the public through the National Technical Information Service, Springfield, VA 22161. <a href="http://www.ntis.gov">http://www.ntis.gov</a>	
19. Security Classif. (of this report) Unclassified	20. Security Classif. (of this page) Unclassified	21. No. of Pages 41	22. Price N/A

## SI\* (MODERN METRIC) CONVERSION FACTORS

### APPROXIMATE CONVERSIONS TO SI UNITS

Symbol	When You Know	Multiply By	To Find	Symbol
<b>LENGTH</b>				
in	inches	25.4	millimeters	mm
ft	feet	0.305	meters	m
yd	yards	0.914	meters	m
mi	miles	1.61	kilometers	km
<b>AREA</b>				
in <sup>2</sup>	square inches	645.2	square millimeters	mm <sup>2</sup>
ft <sup>2</sup>	square feet	0.093	square meters	m <sup>2</sup>
yd <sup>2</sup>	square yard	0.836	square meters	m <sup>2</sup>
ac	acres	0.405	hectares	ha
mi <sup>2</sup>	square miles	2.59	square kilometers	km <sup>2</sup>
<b>VOLUME</b>				
fl oz	fluid ounces	29.57	milliliters	mL
gal	gallons	3.785	liters	L
ft <sup>3</sup>	cubic feet	0.028	cubic meters	m <sup>3</sup>
yd <sup>3</sup>	cubic yards	0.765	cubic meters	m <sup>3</sup>
NOTE: volumes greater than 1,000 L shall be shown in m <sup>3</sup>				
<b>MASS</b>				
oz	ounces	28.35	grams	g
lb	pounds	0.454	kilograms	kg
T	short tons (2,000 lb)	0.907	megagrams (or "metric ton")	Mg (or "t")
<b>TEMPERATURE (exact degrees)</b>				
°F	Fahrenheit	5 (F-32)/9 or (F-32)/1.8	Celsius	°C
<b>ILLUMINATION</b>				
fc	foot-candles	10.76	lux	lx
fl	foot-Lamberts	3.426	candela/m <sup>2</sup>	cd/m <sup>2</sup>
<b>FORCE and PRESSURE or STRESS</b>				
lbf	poundforce	4.45	newtons	N
lbf/in <sup>2</sup>	poundforce per square inch	6.89	kilopascals	kPa
<b>APPROXIMATE CONVERSIONS FROM SI UNITS</b>				
Symbol	When You Know	Multiply By	To Find	Symbol
<b>LENGTH</b>				
mm	millimeters	0.039	inches	in
m	meters	3.28	feet	ft
m	meters	1.09	yards	yd
km	kilometers	0.621	miles	mi
<b>AREA</b>				
mm <sup>2</sup>	square millimeters	0.0016	square inches	in <sup>2</sup>
m <sup>2</sup>	square meters	10.764	square feet	ft <sup>2</sup>
m <sup>2</sup>	square meters	1.195	square yards	yd <sup>2</sup>
ha	hectares	2.47	acres	ac
km <sup>2</sup>	square kilometers	0.386	square miles	mi <sup>2</sup>
<b>VOLUME</b>				
mL	milliliters	0.034	fluid ounces	fl oz
L	liters	0.264	gallons	gal
m <sup>3</sup>	cubic meters	35.314	cubic feet	ft <sup>3</sup>
m <sup>3</sup>	cubic meters	1.307	cubic yards	yd <sup>3</sup>
<b>MASS</b>				
g	grams	0.035	ounces	oz
kg	kilograms	2.202	pounds	lb
Mg (or "t")	megagrams (or "metric ton")	1.103	short tons (2,000 lb)	T
<b>TEMPERATURE (exact degrees)</b>				
°C	Celsius	1.8C+32	Fahrenheit	°F
<b>ILLUMINATION</b>				
lx	lux	0.0929	foot-candles	fc
cd/m <sup>2</sup>	candela/m <sup>2</sup>	0.2919	foot-Lamberts	fl
<b>FORCE and PRESSURE or STRESS</b>				
N	newtons	2.225	poundforce	lbf
kPa	kilopascals	0.145	poundforce per square inch	lbf/in <sup>2</sup>

\*SI is the symbol for International System of Units. Appropriate rounding should be made to comply with Section 4 of ASTM E380. (Revised March 2003)

## TABLE OF CONTENTS

<b>EXECUTIVE SUMMARY .....</b>	<b>1</b>
<b>Purpose of Report .....</b>	<b>1</b>
<b>Methodology .....</b>	<b>1</b>
<b>Key Results .....</b>	<b>2</b>
<b>CHAPTER 1. INTRODUCTION .....</b>	<b>5</b>
<b>Background .....</b>	<b>5</b>
<b>Report Overview .....</b>	<b>6</b>
<b>CHAPTER 2. CAV APPLICATIONS .....</b>	<b>7</b>
<b>CHAPTER 3. DESCRIPTION OF CASE STUDY LOCATION.....</b>	<b>9</b>
<b>CHAPTER 4. MODELING AND SIMULATION .....</b>	<b>11</b>
<b>Modeling Framework for CAVs.....</b>	<b>11</b>
<b>Baseline Strategy Simulation Calibration and Validation .....</b>	<b>11</b>
<b>CAV Functionalities.....</b>	<b>15</b>
<b>CAV Operational Alternatives .....</b>	<b>17</b>
<b>Performance Measures .....</b>	<b>17</b>
<b>CHAPTER 5. SIMULATION AND RESULTS.....</b>	<b>19</b>
<b>Design of Simulation Strategies .....</b>	<b>19</b>
<b>Simulation Results for Different Scenarios .....</b>	<b>19</b>
CACC Effects at Different Market Penetration Rates .....	19
VAD Effects at Different Market Penetration Rates .....	21
Effects of Applying a CAV-Only ML .....	23
Effects of Traffic Demand Increase .....	25
<b>Results Discussion .....</b>	<b>27</b>
<b>CHAPTER 6. CONCLUSIONS.....</b>	<b>29</b>
<b>Summary of Study Findings .....</b>	<b>29</b>
<b>Summary of Impacts.....</b>	<b>30</b>
<b>Limitations of the Study and Suggestions for Additional Research.....</b>	<b>31</b>
<b>REFERENCES.....</b>	<b>33</b>

## LIST OF FIGURES

Figure 1. Illustration. SR 99 study corridor south of Sacramento, CA.....	9
Figure 2. Diagram. Structure of human-driver model. <sup>(14)</sup> .....	12
Figure 3. Equation. GEH statistic calculation.....	13
Figure 4. Equation. MAPE parameter calculation.....	13
Figure 5. Diagram. Car-following and lane-changing dynamics of CACC vehicles. <sup>(14)</sup> .....	16
Figure 6. Equation. $\bar{v}$ calculation.....	17
Figure 7. Equation. $\overline{mpg}$ calculation.....	18
Figure 8. Equation. $P_{string}$ calculation. ....	18
Figure 9. Equation. $L_{string}$ calculation.....	18
Figure 10. Graph. $\bar{v}$ and $\overline{mpg}$ under various CACC market penetration rates. ....	20
Figure 11. Graph. $P_{string}$ and $L_{string}$ under various CACC market penetration rates.....	21
Figure 12. Chart. $\bar{v}$ under various VAD market penetration rates.....	22
Figure 13. Chart. $\overline{mpg}$ under various VAD market penetration rates.....	22
Figure 14. Chart. $P_{string}$ under various VAD market penetration rates. ....	23
Figure 15. Chart. $L_{string}$ under various VAD market penetration rates.....	23
Figure 16. Graph. $\bar{v}$ under the influence of VADs and MLs.....	24
Figure 17. Graph. $\overline{mpg}$ under the influence of VADs and MLs. ....	24
Figure 18. Graph. $\bar{v}$ with and without demand increase.....	25
Figure 19. Graph. $\overline{mpg}$ with and without demand increase. ....	26

## LIST OF TABLES

Table 1. GEH results.....	14
Table 2. MAPE results.....	14
Table 3. Study strategy definition.....	19
Table 4. $\bar{v}$ (mph) under different traffic demand inputs.....	26

## LIST OF ABBREVIATIONS

ACC	adaptive cruise control
ATM	active traffic management
CACC	cooperative adaptive cruise control
Caltrans	California Department of Transportation
CAV	connected automated vehicle
CF	car-following
CRM	coordinated ramp metering
DLC	discretionary lane-change
GEH	Geoffrey E. Havers
HOV	high-occupancy vehicle
I2V	infrastructure-to-vehicle
LC	lane-changing
LRRM	local responsive ramp metering
MAPE	mean absolute percentage error
ML	managed lane
MLC	mandatory lane-changing
mpg	miles per gallon
NGSIM	Next Generation SIMulation
PeMS	Performance Measurement System
RM	ramp meter
TMC	traffic management center
V2V	vehicle-to-vehicle
VAD	vehicle awareness device
VHT	vehicle hours traveled
VMT	vehicle miles traveled
VSA	variable speed advisory
VSL	variable speed limit
V2I	vehicle-to-infrastructure

## **EXECUTIVE SUMMARY**

### **PURPOSE OF REPORT**

The purpose of this report is to document a simulation-based case study investigating the effectiveness of SAE Level 1 automation technology for mitigating or solving existing transportation problems related to congestion, fuel consumption, and emissions.<sup>(1)</sup> Specifically, the report documents traffic simulation results and analyses for a set of strategies conducted on a 13-mi segment of the SR 99 corridor (since only the northbound side was studied, any reference to the corridor is in reference to just the northbound side) in California from Elk Grove Boulevard to SR 50 near Sacramento. This case study examined the impacts of cooperative adaptive cruise control (CACC)-equipped vehicle (CACC vehicle hereafter) string operations on traffic performance and fuel consumption for the busy urban corridor. The study analyzed performance on this 13-mi corridor under various CACC market penetration scenarios, traffic demand inputs, and CACC management strategies. Specifically, the research team examined average vehicle speed, average miles per gallon (mpg) of fuel consumed, average string length, and CACC vehicle string probability (i.e., the probability of a CACC vehicle operating in a string) at various CACC market penetration rates (i.e., baseline, 20, 40, 60, 80, and 100 percent). The study investigated the corridor's spatiotemporal traffic patterns under the existing traffic demand and a 20-percent traffic demand increase. Additionally, it analyzed CACC string operation after vehicle awareness device (VAD) and CACC managed lane (ML) strategies were implemented.

### **METHODOLOGY**

The freeway corridor simulated in this study is one of the major commuting routes that connect downtown Sacramento to suburban residential areas. The study only simulated the corridor's northbound direction. There is extensive traffic congestion during the morning peak hours of 6:30 am to 9:00 am on this segment of the freeway. The congested areas are isolated at five on-ramp bottlenecks during the beginning of the morning peak hours. However, as the congestion builds, the queues at most downstream bottlenecks propagate backward and eventually connect to the upstream bottlenecks. This congestion accumulation causes traffic breakdown on the entire corridor. The study is based on the hypothesis that CACC string operations can mitigate the corridor's heavy congestion.

This case study used microscopic traffic simulation models to depict the impacts of CACC. The modeling framework was based on a state-of-the-art human-driver model and an adaptive cruise control (ACC) and CACC car-following model. The human-driver model was calibrated using traffic data collected from the study corridor, and the ACC and CACC car-following models were calibrated using ACC and CACC trajectory data obtained in field tests. The research team tested the ACC and CACC model against the trajectory data obtained from a real-world CACC string.

The study examined the corridor's traffic performance and fuel consumption under four CACC implementation strategies. The experiments conducted in the four strategies analyzed the impacts of CACC with or without ML and VAD operations implemented at different traffic congestion levels. Strategy 1 investigated the influence of CACC string operation under various CACC and

VAD market penetration rates. Strategy 2 investigated the same scenarios as strategy 1 but also implemented the ML strategy. Strategy 3 also analyzed the same scenarios as strategy 1 but with a 20-percent traffic demand increase for the entire corridor. Strategy 4 investigated the same scenarios as strategy 2 but with a 20-percent traffic demand increase. The experiments conducted in the four strategies analyzed the impacts of CACC with or without CACC ML and VAD implementation under different traffic congestion levels.

## **KEY RESULTS**

The case study revealed that the average speed of the study corridor increased linearly with CACC market penetration. The average speed increased by 70 percent (from 34 to 56 mph) at 100-percent CACC market penetration compared to the baseline strategy (i.e., 0-percent CACC market penetration). The CACC application positively impacted fuel efficiency, with the highest average fuel efficiency of 26 mpg achieved in the 30-percent CACC market penetration scenario. This efficiency was 5 percent higher than the baseline strategy. As CACC market penetration reached 100 percent, the fuel efficiency dropped to 22 mpg, which was 11 percent lower than the baseline fuel efficiency level. The CACC string operation improved fuel efficiency in the low to medium CACC market penetration scenarios because it mitigated traffic congestion. As traffic flow became more stable at 20- to 40-percent market penetration rates, overall fuel efficiency improved. When CACC market penetration exceeded 40 percent, traffic flow ran at a higher speed, which reduced the fuel efficiency improvement.

When CACC market penetration reached 100 percent, the corridor allowed about 30 percent more traffic to enter the network with no reduction in travel time. This increase was lower than the capacity increase (i.e., 90 percent) that could be achieved at an isolated bottleneck. The performance improvement of an upstream isolated bottleneck increased output flow to downstream segments, which led to mobility reduction at downstream bottlenecks. As a result, improving isolated bottlenecks did not necessarily bring about a benefit of the same magnitude for the entire corridor. This observation indicated a need to develop corridor-level traffic flow-management strategies (e.g., speed harmonization) to coordinate the input and output flow of each bottleneck.

The analysis results showed that CACC string probability was only 80 percent, even when all vehicles were equipped with CACC. This probability indicated a need for local or systematic string strategies that would help isolated CACC vehicles form strings. Once the current ad hoc string scheme is replaced by those strategies, the string performance should substantially increase, leading to enhanced traffic flow.

This case study considered VAD and ML strategies. The VAD strategy enhanced CACC string operation by increasing string probability. The CACC vehicles located string leaders more easily since more manually driven vehicles were equipped with VAD. The strategy had the most influence when CACC market penetration was at 20 or 40 percent. In those scenarios, the average speed increased by 8 percent and fuel efficiency remained nearly constant. When CACC market penetration increased, CACC vehicles found CACC string leaders more easily, reducing the effect of the VAD strategy. However, the ML strategy decreased corridor performance when implemented alone. When the strategy was active, it caused CACC vehicles to make lane changes to merge into the ML. These lane changes disturbed the general-purpose lanes, making

the traffic flow in the general-purpose lanes unstable. A potential solution to this challenge could be using dedicated on-ramps that allow CACC vehicles to enter the ML directly.



## CHAPTER 1. INTRODUCTION

### BACKGROUND

For now, the best way to understand the impact of connected automated vehicle (CAV) technology on traffic mobility, energy consumption, and emission is through microscopic simulations that properly model the dynamic interactions between CAVs and manually driven vehicles. This understanding can be achieved by testing CAVs in public traffic and using the test data to develop models because high CAV market penetration does not exist in practice and will not exist for about a decade. Therefore, such data cannot be collected for mixed-traffic (i.e., manually driven vehicles and CAVs) modeling. To this end, FHWA has sponsored three case studies (I-66, SR 99, and Traffic Optimization for Signalized Corridors) under this project to investigate the traffic and energy impacts of CAV and the bundled applications of CAV and traffic management strategies on various freeway and arterial corridors.

The SR 99 case study that was part of this project examined the impact of cooperative adaptive cruise control (CACC)-equipped vehicle (CACC vehicle hereafter) string operation on traffic performance and fuel consumption on a 13-mi segment of the SR 99 corridor in California from Elk Grove Boulevard to SR 50 near Sacramento. The corridor is one of the major commuting routes that connect downtown Sacramento with suburban residential areas. This study only simulated the corridor's northbound direction. There is extensive traffic congestion during the morning peak hours on this segment of the freeway. The congested areas are isolated at five on-ramp bottlenecks during the beginning of the morning peak hours. However, as congestion builds, the queues at most downstream bottlenecks propagate backward and eventually connect with the upstream bottlenecks. This congestion accumulation causes traffic breakdown on the entire corridor. The study corridor is managed and operated by the California Department of Transportation (Caltrans). As an agency, Caltrans is committed to continually improving its transportation systems. Technologies such as CAVs show promise for improving the safety, efficiency, and environmental impacts of travel on California freeways. Thus, Caltrans is interested in quantifying the possibility of using CAVs to improve the corridor's performance. The agency identified the specific simulation scenarios and strategies they were interested in. This case study evaluated those strategies.

CACC string operations may be able to mitigate the heavy congestion on the study corridor. Previous studies indicated that freeway pipeline capacity can increase by 96 percent as CACC market penetration rates rise from baseline to 100 percent.<sup>(2)</sup> CACC can reduce or eliminate congestion because CACC vehicles travel in a string and adopt shorter than normal gaps in the car-following mode. This behavior results in saving time-space resources offered by the freeway facility. CACC vehicles also improve the overall performance of the traffic stream when they form strings because they react to traffic disturbances collectively, damping traffic waves and enhancing flow stability. Additionally, the CACC controller responds to the preceding CACC vehicle's speed changes more quickly than human drivers. This fast reaction allows traffic flow to return to high throughput after it is interrupted.

The probability of a CACC vehicle operating in a string (string probability hereafter) is associated with CACC market penetration rates. It can be difficult for a CACC vehicle to identify a string leader at low market penetration rates. This challenge can be improved by CACC management strategies that increase local string probabilities. To address this challenge, the study investigated two management strategies. The first one installed vehicle awareness devices (VADs) on manually driven vehicles. The device offered connectivity to the manually driven vehicles, allowing them to become CACC string leaders. When VAD penetration rates increase, isolated CACC vehicles can identify string leaders more easily, thus creating more strings in the traffic stream. The second strategy converted existing carpool lanes or express lanes to CACC managed lanes (MLs). This approach created a pure CACC environment in the ML, allowing vehicles driving in those lanes to form strings while performing car following. The study assessed the effectiveness of VAD and ML strategies on a complicated freeway corridor. The analysis results could help local agencies develop field implementation plans for these strategies.

## **REPORT OVERVIEW**

Chapter 1 has provided an introduction and overview of the case study. The remainder of the report is structured as follows:

- Chapter 2 provides a review of the CACC technology tested in the case study.
- Chapter 3 describes the network, travel patterns, and existing traffic control and management strategies of the SR 99 corridor.
- Chapter 4 gives detailed information on traffic simulation models used to depict CACC string operation, interaction among CACC vehicles and manually driven vehicles, and CACC management strategies.
- Chapter 5 discusses the simulation results.
- Chapter 6 summarizes the study findings and presents concluding remarks.

## CHAPTER 2. CAV APPLICATIONS

CACC technology combines adaptive cruise control (ACC) with wireless communication, allowing vehicles to share data among themselves and with the infrastructure. This cooperative form of vehicle-to-vehicle communication enables CACC vehicles to follow each other more accurately and closely than conventional ACC. As a result, it also significantly improves traffic flow stability (i.e., damping out shock waves) and allows drivers to use the automatic car-following function safely and comfortably at shorter gap settings. These shorter gaps make it possible to almost double the capacity per freeway lane while also improving driver satisfaction (i.e., avoiding more cut-ins and feeling more confident in the system because it provides braking action as soon as brake lights illuminate on the preceding vehicle). The vehicle-to-infrastructure communications that CACC allows can promote speed harmonization on freeways in response to traffic conditions, improve traffic flow stability and throughput, and reduce the start-up delays among strings of vehicles that are stopped in the congested roads. Both CACC applications reduce the energy and environmental impacts of road transportation by reducing traffic flow disturbances (i.e., stop-and-go traffic).

A successful CACC management strategy can increase the probability for individual CACC vehicles to join strings. Once a string is formed, the strategy can also help maintain the string operation throughout a freeway corridor. Larson et al. proposed a strategy that applied high-level coordination to allow CACC vehicles to form strings at individual freeway entrances based on their origin and destination.<sup>(3,4)</sup> Liang et al. created a strategy for sending acceleration or deceleration instructions to CACC vehicles in the traffic stream so they can match dynamically with each other.<sup>(5)</sup> These two strategies require traffic management centers (TMCs) or roadside units to perform string formation as the individual vehicles are unable to form the string by themselves. They might not be implemented in the field until a substantial portion of the vehicle fleet adopts CACC.

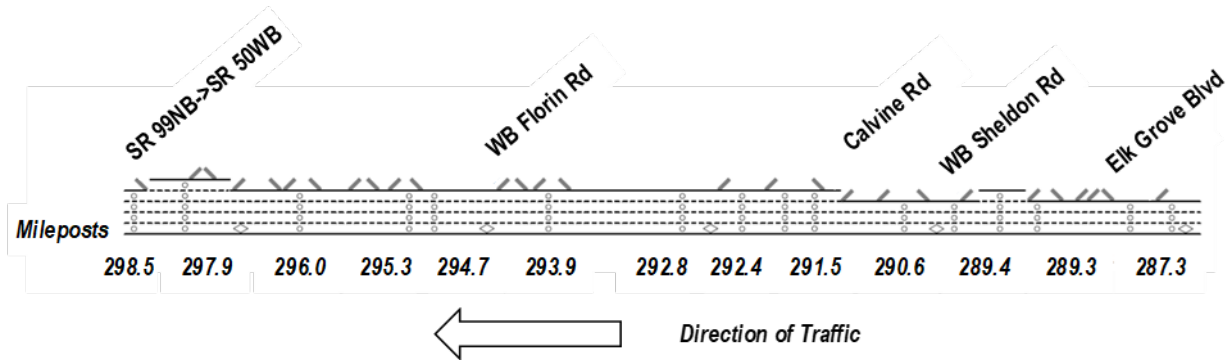
Currently, there are measures that can be taken to achieve better CACC string operation. For example, implementing a CACC-eligible ML (which includes CACC and VAD strategies, CACC ML hereafter) can slightly prevent CACC traffic flow from being interrupted by manually driven vehicles. As CACC vehicles concentrate in the ML, the probability of string formation increases. Transportation management centers can also encourage manually driven vehicles to adopt VADs. This strategy increases the probability of CACC vehicles operating in strings because it allows a CACC vehicle to join a string led by a VAD-equipped vehicle (VAD vehicle hereafter).<sup>(6)</sup> Another potential strategy is to use on-board human-machine interfaces to discourage CACC drivers from making discretionary lane changes to increase the amount of time vehicles stay in the string. Since these strategies require little upgrade to existing freeway infrastructure, they can be implemented in the field as CACC vehicles first emerge in the traffic stream.

The research team narrowed this study's consideration to the impact analysis of strategies likely to be implemented near-term and that will not require major upgrades to existing road infrastructure. The CACC management strategies analyzed in this study are as follows:

- Implementing a VAD strategy on manually driven vehicles. VAD vehicles have wireless communication capability and as such can broadcast real-time information regarding their operation status and route choice. Although they do not have an automated controller to perform the car-following task, they can serve as a CACC vehicle string leader. This strategy increases the probability of CACC vehicles traveling in CACC mode and thus offers an incentive for users to equip their vehicles with CACC, even at low CACC market penetration rates.
- Implementing a CACC ML strategy. The ML strategy has been used widely to serve high-occupancy vehicles (HOVs) or drivers willing to pay a toll with the purpose of improving overall efficiency of the freeway system. The CACC ML strategy adopts a similar operational concept that only allows CACC vehicles and VAD vehicles to enter the ML, which physically separates the CACC traffic stream and the regular traffic stream. As the CACC and VAD vehicles concentrate in the ML, the probability of traveling in CACC strings increases. The ML also reduces interaction between CACC vehicles and manually driven vehicles so CACC strings are less likely to be interrupted in the ML.

### CHAPTER 3. DESCRIPTION OF CASE STUDY LOCATION

The SR 99 corridor to the south of Sacramento was selected as the case study segment. The segment is 13 mi long, starting at the Elk Grove Boulevard on-ramp and extending to the SR 50 off-ramp. This segment contains 16 on-ramps and 12 off-ramps. The plot in figure 1 shows the lane configuration. The segment also contains nine interchanges with local arterial streets and an interchange with a major urban freeway. These interchanges include four partial cloverleaf interchanges, three full cloverleaf interchanges, two diamond interchanges with local arterials, and a directional interchange with a freeway. Furthermore, the study corridor contains three lanes (one HOV lane and two general-purpose lanes) upstream of the Calvine Road interchange. There is an additional general-purpose lane downstream of that interchange. The on-ramp merging and weaving sections located downstream of the Elk Grove Boulevard interchange, as well as the off-ramp at the SR 50 interchange, contribute to the recurrent traffic congestion observed during the morning peak hours in this corridor. The morning peak hours begin at 6:30 a.m. and end at 9:00 a.m. and the traffic congestion is a result of the high suburb-to-downtown traffic. During the morning peak hours, the vehicle fleet is usually composed of 97 percent passenger vehicles and 3 percent trucks and transit vehicles. At the beginning of the congestion period, isolated bottlenecks usually form at the SR 50, westbound Florin Road, and Calvine Road on-ramps. The congested traffic at these bottlenecks gradually propagates upstream and triggers traffic breakdown at minor upstream bottlenecks. The traffic congestion affects the entire corridor from 7:00 a.m. to 8:30 a.m. The queue discharging rate at each bottleneck ranges from 1,600 to 1,800 vehicles per hour per lane.



Source: FHWA.  
NB = northbound; WB = westbound.

**Figure 1. Illustration. SR 99 study corridor south of Sacramento, CA.**

The study corridor on-ramps use local responsive ramp metering (LRRM) and coordinated ramp metering (CRM) algorithms to control the flow of on-ramp traffic and mitigate peak-hour congestion.<sup>(7)</sup> The research team used the LRRM algorithm for the five upstream on-ramps starting at the beginning of the corridor—note that some interchanges have several on-ramps. The research team implemented an optimized CRM algorithm for the 11 downstream ramp meters (RMs). The algorithms are different in that the LRRM algorithm determines the RM rate for an on-ramp based only on the local mainline occupancy and flow of its immediate upstream mainline detectors, whereas the CRM algorithm determines the RM rate by considering mainline occupancy and flow of the whole corridor as well as the demand at all on-ramps.

The CRM algorithm implemented in this corridor was based on an optimal control approach.<sup>(7)</sup> The objective function was the difference between total vehicle hours traveled (VHT) and total vehicle miles traveled (VMT):  $VHT - \alpha VMT$ , where  $\alpha$  is a positive number that converts VMT into VHT. The VHT term in the objective function allows the CRM algorithm to minimize overall freeway mainline travel time. However, if there is no VMT value, the CRM algorithm will execute the lowest RM rate, which causes an excessive delay for on-ramp traffic. To address this problem, the objective function also includes the negative VMT value. This value allows the system to maximize VMT by encouraging as many on-ramp vehicles to enter the freeway as possible. The algorithm was implemented to control the SR 99 corridor as a long discharging section in the regard that, on average, downstream traffic should not be more congested than upstream traffic. The research team found that this was the best way to discharge overall traffic in the fastest manner.

The SR 99 corridor has an exclusive HOV lane adjacent to the median with continuous access and egress that operates only from 6:00 a.m. to 10:00 a.m. Data from both free-flow and congested-flow traffic were obtained from the Caltrans Performance Measurement System (PeMS) to depict recurrent congestion and provide sufficient data for model calibration.<sup>(8)</sup> The empirical data revealed a complex congestion pattern with interacting bottlenecks during the morning peak hours and showed propagation and recovery of the congestion.

## CHAPTER 4. MODELING AND SIMULATION

This chapter provides a brief introduction of the simulation models used for depicting car-following and lane-changing behaviors of human drivers and CAVs. The chapter also presents model calibration and validation results to demonstrate the explanatory capability of the models.

### MODELING FRAMEWORK FOR CAVs

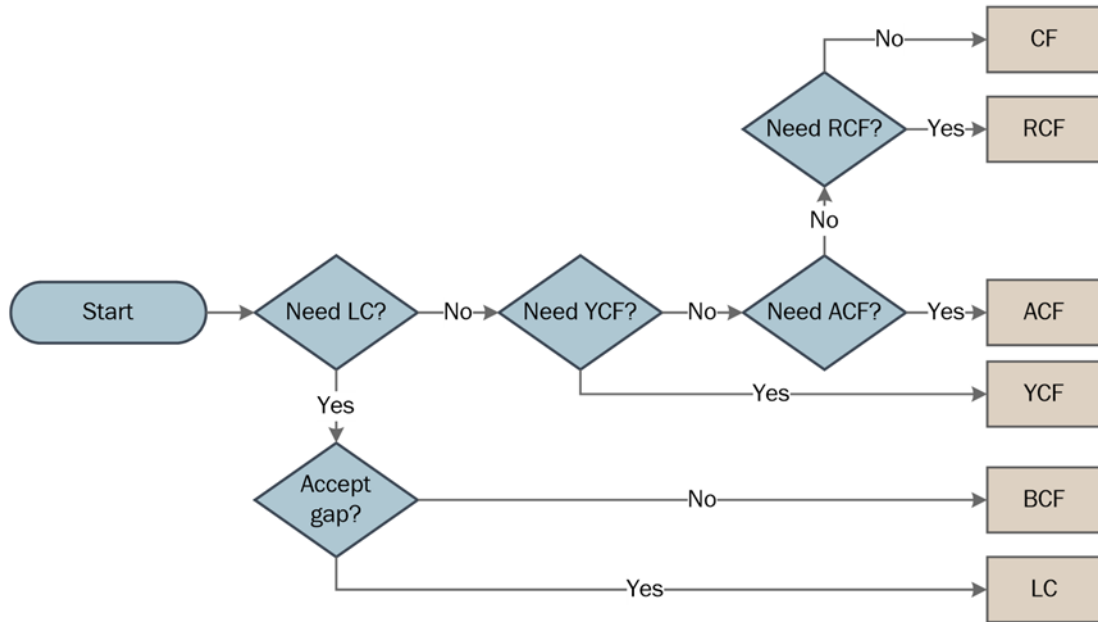
The modeling framework used in this case study was based on the Next Generation SIMulation (NGSIM) oversaturated-flow human-driver model reported in Yeo et al. and the ACC and CACC car-following model based on ACC and CACC field test data.<sup>(9-11)</sup> The human-driver model was calibrated using field data collected from the study corridor, and its modeling capability was cross-validated with the Microscopic Open Traffic Simulation model.<sup>(12,13)</sup> The ACC and CACC model was tested against trajectory data obtained from a real-world CACC string.<sup>(11)</sup> Liu et al. describe the lane-changing behaviors of CACC vehicles and the algorithms for implementing VAD and ML strategies.<sup>(14)</sup> The simulation framework and the study corridor were implemented in Aimsun® via its application program interface.<sup>(15)</sup> The research team adopted the built-in demand generation functions of the simulation tool to provide various traffic demand inputs for the freeway network.

### BASELINE STRATEGY SIMULATION CALIBRATION AND VALIDATION

The baseline simulation model depicts the behaviors of human drivers. Microscopic human-driver car-following behavior and human-driven vehicle interactions with nearby vehicles determine the overall traffic pattern at the macroscopic level. The human-driver model that describes such driver interactions was built on the basic framework of the NGSIM oversaturated flow model proposed by Yeo et al.<sup>(9)</sup> The research team made extensions and modifications to depict car-following and lane-changing behaviors that were not represented in the original model. In the proposed model, the driver's car-following and lane-changing behaviors are partitioned into the following fundamental driving modes:

- Regular car-following mode.
- Lane-change mode, which includes discretionary lane change, active lane change, and mandatory lane change.
- After lane-changing car-following mode in which a driver temporarily adopts a short gap after a lane-change maneuver.
- Before lane-changing car-following mode in which a driver speeds up or slows down to align with an acceptable gap in the target lane.
- Receiving car-following mode in which a driver temporarily adopts a short gap after a vehicle from the adjacent lane merges in front.
- Yielding (cooperative) car-following mode.

As depicted in figure 2, at the beginning of each simulation update interval, the subject driver determines the driving mode based on a set of car-following and lane-changing rules. Each driving mode is associated with specific car-following and lane-changing algorithms that are used to determine the driver's speed and position at the end of the update interval. The update process is then executed iteratively for every modeled vehicle in the simulation environment, resulting in a trajectory for each vehicle over the simulation period.



Source: FHWA.

ACF = after lane-changing car-following mode; BCF = before lane-changing car-following mode; CF = car-following mode; LC = lane-change mode; RCF = receiving car-following mode; YCF = yielding (cooperative) car-following mode.

**Figure 2. Diagram. Structure of human-driver model.<sup>(14)</sup>**

The human-driver models depict car-following and lane-changing behaviors of passenger vehicles and heavy-duty trucks. For passenger vehicles, the models are applied to conventional, manually driven vehicles; VAD vehicles; and ACC and CACC vehicles when they are not operating under the ACC and CACC mode. Truck behavior is always modeled by the human-driver models. This study did not consider truck platooning scenarios. All trucks are assumed to be manually driven.

The human-driver model was calibrated and validated by the research team's previous study.<sup>(16)</sup> The empirical data collected on the SR 99 corridor were used to calibrate the baseline model. The considered period was from 4:00 a.m. to 12:00 p.m. Loop detector data for this period were obtained from the Caltrans PeMS, which provided 5-min flow and speed data for each lane on the corridor's mainline. The calibrated model accurately reproduced the study corridor's speed and flow patterns. The model's goodness-of-fit was measured by two indicators, the Geoffrey E. Havers (GEH) statistic and the mean absolute percentage error (MAPE).<sup>(17)</sup>

The GEH statistic is computed using the equation shown in figure 3.

$$GEH(k) = \sqrt{\frac{2[M(k) - C(k)]^2}{M(k) + C(k)}}$$

**Figure 3. Equation. GEH statistic calculation.**

Where:

$GEH(k)$  = discrepancy between simulated and measured flow during the  $k$ th time interval (vehicles per hour).

$M(k)$  = simulated flow during the  $k$ th time interval (vehicles per hour).

$C(k)$  = flow measured in the field during the  $k$ th time interval (vehicles per hour).

The flow MAPE is defined by the equation shown in figure 4.

$$MAPE = \frac{1}{N \cdot T} \sum_{n=1}^N \sum_{t=1}^T \frac{M_{n,t}^{real} - M_{n,t}^{sim}}{M_{n,t}^{real}}$$

**Figure 4. Equation. MAPE parameter calculation.**

Where:

$N$  = number of detectors.

$T$  = number of time intervals.

$M_{n,t}^{real}$  = field observed data of detector  $n$  obtained during time interval  $t$ .

$M_{n,t}^{sim}$  = simulated data (i.e., flow) of detector  $n$  obtained during time interval  $t$ .

The simulated flow is acceptable based on the following parameters:

- The average GEH of all detectors should be less than a threshold of 5 The simulated flow passes the calibration condition if  $GEH(k) < 5$  for more than 85 percent of all 5-min time intervals.
- The MAPE is less than 10 percent.

The model validation results are shown in table 1 and table 2.

**Table 1. GEH results.**

<b>Detector Location (Milepost)</b>	<b>Target</b>	<b>Percentage Met</b>	<b>Target Met?</b>
287.3	GEH < 5 for >85% of <i>k</i>	100.00	Yes
287.6	GEH < 5 for >85% of <i>k</i>	97.92	Yes
289.3	GEH < 5 for >85% of <i>k</i>	98.65	Yes
289.4	GEH < 5 for >85% of <i>k</i>	98.54	Yes
290.0	GEH < 5 for >85% of <i>k</i>	98.65	Yes
290.7	GEH < 5 for >85% of <i>k</i>	97.71	Yes
291.5	GEH < 5 for >85% of <i>k</i>	93.54	Yes
291.9	GEH < 5 for >85% of <i>k</i>	91.04	Yes
292.4	GEH < 5 for >85% of <i>k</i>	93.23	Yes
292.8	GEH < 5 for >85% of <i>k</i>	93.13	Yes
294.0	GEH < 5 for >85% of <i>k</i>	92.81	Yes
294.7	GEH < 5 for >85% of <i>k</i>	94.79	Yes
295.3	GEH < 5 for >85% of <i>k</i>	94.90	Yes
296.0	GEH < 5 for >85% of <i>k</i>	88.65	Yes
297.9	GEH < 5 for >85% of <i>k</i>	79.27	No
298.5	GEH < 5 for >85% of <i>k</i>	92.50	Yes
<b>Overall</b>	<b>GEH &lt; 5 for &gt;85% of <i>k</i></b>	<b>94.08</b>	<b>Yes</b>

**Table 2. MAPE results.**

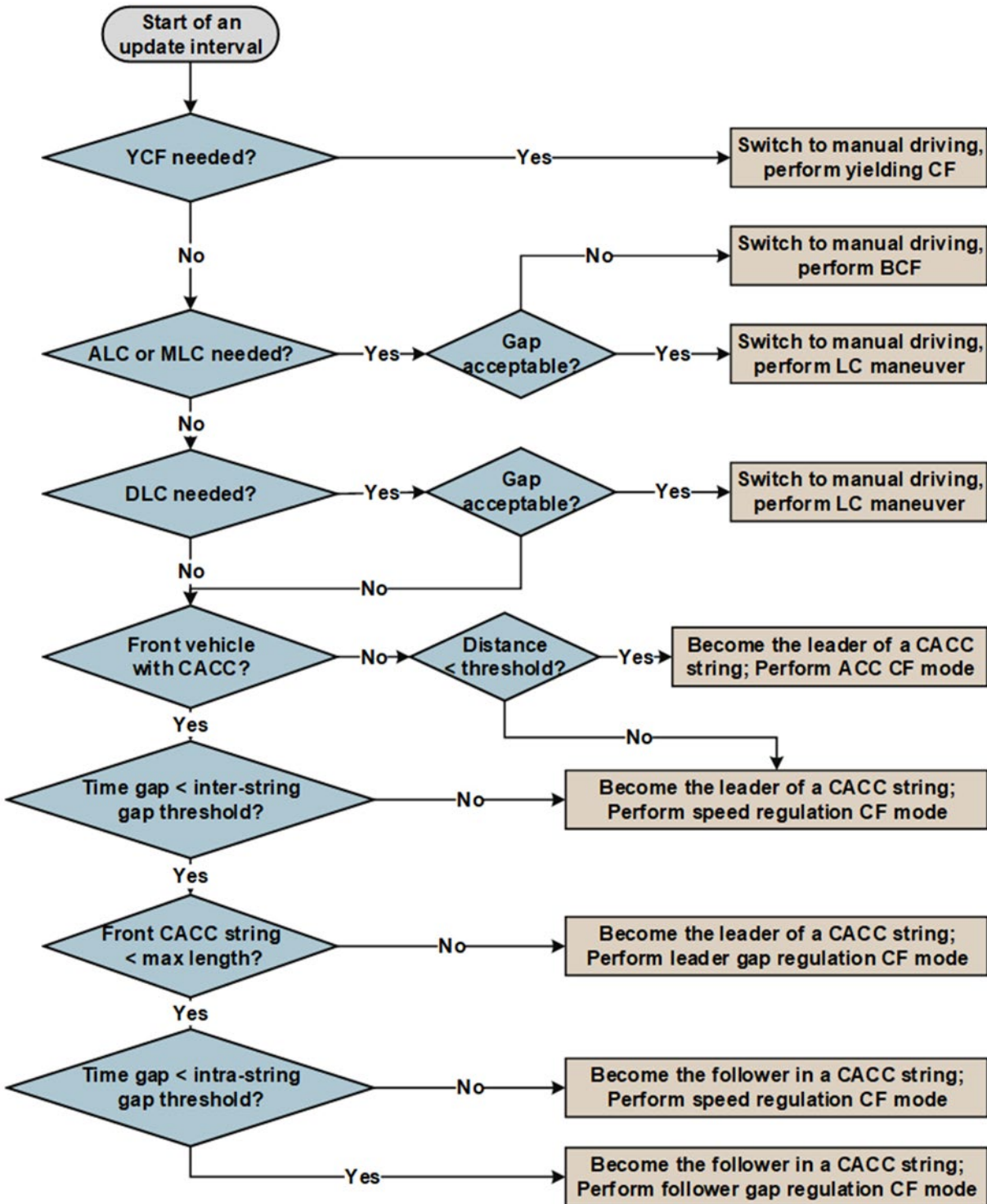
<b>Detector Location (Milepost)</b>	<b>Target</b>	<b>Percentage Error</b>	<b>Target Met?</b>
287.3	MAPE < 10%	1.99	Yes
287.6	MAPE < 10%	9.36	Yes
289.3	MAPE < 10%	9.17	Yes
289.4	MAPE < 10%	8.61	Yes
290.0	MAPE < 10%	6.85	Yes
290.7	MAPE < 10%	7.41	Yes
291.5	MAPE < 10%	9.92	Yes
291.9	MAPE < 10%	10.38	No
292.4	MAPE < 10%	8.98	Yes
292.8	MAPE < 10%	8.02	Yes
294.0	MAPE < 10%	8.37	Yes
294.7	MAPE < 10%	7.37	Yes
295.3	MAPE < 10%	8.01	Yes
296.0	MAPE < 10%	10.52	No
297.9	MAPE < 10%	14.20	No
298.5	MAPE < 10%	14.09	No
<b>Overall</b>	<b>MAPE &lt; 10%</b>	<b>8.21</b>	<b>Yes</b>

Because the SR northbound 99 corridor is a complex freeway segment, the research team qualitatively checked the speed contour plots to determine the model's ability to generate realistic speed patterns. In the previous calibration, the simulation model reproduced traffic congestion consistent with real-world observations. This case study included the CRM algorithm, which the research team did not consider in the previous calibration. Although the algorithm had little impact on the overall simulated 5-min flow that was previously calibrated, it affected spatiotemporal speed variations at local bottlenecks. For this reason, the research team slightly adjusted the simulation models to generate speed contour plots that matched the field data. The following parameters were changed from the original levels as shown:

- Reaction time—0.8 s to 1.0 s.
- Maximum comfortable vehicle acceleration—6.56 ft/s<sup>2</sup> to 3.94 ft/s<sup>2</sup>.
- Maximum comfortable vehicle deceleration—13.12 ft/s<sup>2</sup> to 9.84 ft/s<sup>2</sup>.
- Average desired time headway—1.4 s to 1.2 s.

### **CAV FUNCTIONALITIES**

This study adopted the models developed in Milanés and Shladover to depict ACC and CACC car-following behaviors.<sup>(10,11)</sup> CACC vehicles exhibit significantly different car-following behavior from manual drivers and form strings that allow them to follow the preceding vehicles with short gaps. CACC vehicle drivers can also exit their closely coupled string and turn off CACC to change lanes or exit the freeway. The proposed CACC and ACC vehicle-behavior model depicts the lane-changing behaviors of CACC and ACC drivers. The CACC vehicle modeling framework is highlighted in figure 5. Although CACC system implementation relies on information received from the leading vehicle in the CACC string as well as from the immediately preceding vehicle, the empirical models used in the simulation provided a simplified description of the closed-loop, vehicle-following dynamics that were achieved relative to the immediately preceding vehicle. This simplified approach is suitable for modeling a large number of CACC vehicles.



Source: FHWA.

ACF = after lane-changing car-following mode; ALC = active lane change; BCF = before lane-changing car-following mode; CF = car-following mode; DLC; discretionary lane change; LC = lane-change mode; MLC = mandatory lane change; RCF = receiving car-following mode; YCF = yielding (cooperative) car-following model.

**Figure 5. Diagram. Car-following and lane-changing dynamics of CACC vehicles.<sup>(14)</sup>**

## CAV OPERATIONAL ALTERNATIVES

This research considered VAD and ML strategies for enhancing CACC string operation along the study corridor. The human-driver models discussed in previous sections are used to depict the behavior of VAD vehicles. In this strategy, the car-following and lane-changing behaviors of VAD vehicle drivers are the same as drivers of conventional vehicles. Even when the VAD vehicle is leading a CACC vehicle string, the target driver may still have a delayed response or make discretionary lane changes toward a faster lane. To capture VAD vehicle connectivity, the study implemented a communication module that allows CACC vehicles within 1,000 ft of a host VAD to receive its real-time speed, location, and acceleration information. The model implementation assumed a perfect communication environment that enabled CACC vehicles to receive VAD information without communication delay or packet loss as long as the CACC vehicle was in communication range.

The CACC ML strategy utilizes the anticipatory lane-changing model the research team developed in a previous study.<sup>(13)</sup> When the strategy is active, it motivates CACC vehicles entering from an on-ramp to merge into the ML if the average speed of the ML was higher than the speed of the general-purpose lane. This motivation causes the CACC drivers to exhibit anticipatory lane-changing behavior—they actively search for downstream gaps for making lane changes. Until they find one, they usually accept smaller car-following gaps and higher desired speed to increase the probability of identifying an acceptable gap. CACC vehicles use manual driving mode to make anticipatory lane changes. As such, the vehicles are temporarily unable to perform CACC string operation. Though the ML attracts CACC vehicles, it does not allow manually driven vehicles to merge into it. This behavior creates a dedicated lane for CACC vehicles only.

## PERFORMANCE MEASURES

The average vehicle speed ( $\bar{v}$ ) is used to depict the traffic performance of the study corridor. The average speed is computed as shown in figure 6.

$$\bar{v} = \frac{\sum VMT}{\sum VHT}$$

**Figure 6. Equation.  $\bar{v}$  calculation**

Where:

$\sum VMT$  = total vehicle miles traveled.

$\sum VHT$  = total vehicle hours traveled.

The average miles per gallon (mpg) of fuel consumed is used to depict the fuel efficiency of the freeway corridor. The mpg results were calculated using the Virginia Tech Comprehensive Power-Based Fuel Consumption Model.<sup>(16)</sup> The average mpg ( $\overline{mpg}$ ) calculation is shown in figure 7.

$$\overline{mpg} = \frac{\sum VMT}{\sum fuel}$$

**Figure 7. Equation.  $\overline{mpg}$  calculation.**

Where  $\sum fuel$  is the total amount of fuel consumed by the simulated vehicles.

The benefit CACC passenger vehicles offer is attributable to CACC string operation. This benefit is unlike CACC trucks, for which the benefit is attributable to both CACC string operation and the aerodynamic drag reduction. There is negligible aerodynamic drag reduction for CACC strings with passenger vehicles. As a result, this study did not account for fuel savings from aerodynamic drag. The research applies average string probability ( $P_{string}$ ) and average string length ( $L_{string}$ ) to describe string performance. The calculation of these two parameters are shown in figure 8 and figure 9:

$$P_{string} = \frac{N_{vehicles\ in\ string}}{N_{CACC}}$$

**Figure 8. Equation.  $P_{string}$  calculation.**

$$L_{string} = \frac{N_{vehicles\ in\ string}}{N_{string}}$$

**Figure 9. Equation.  $L_{string}$  calculation.**

Where:

$N_{vehicles\ in\ string}$  = number of vehicles operating in the string.

$N_{CACC}$  = number of CACC vehicles in the network.

$N_{string}$  = number of CACC strings in the network.

## CHAPTER 5. SIMULATION AND RESULTS

### DESIGN OF SIMULATION STRATEGIES

This study examined traffic performance and fuel consumption on the SR 99 corridor under four CACC implementation strategies shown in table 3.

**Table 3. Study strategy definition.**

Strategy	Scenario ID	Demand Increase (%)	CACC Market Penetration Rate (%)	VAD Market Penetration Rate (%)	ML
1	1–6	0	0, 20, 40, 60, 80, 100	0	No
1	7–10	0	20, 40, 60, 80	30	No
1	11–14	0	20, 40, 60, 80	70	No
1	15–18	0	20, 40, 60, 80	100	No
2	19–22	0	20, 40, 60, 80	0	Yes
2	23–26	0	20, 40, 60, 80	30	Yes
2	27–30	0	20, 40, 60, 80	70	Yes
2	31–34	0	20, 40, 60, 80	100	Yes
3	35–40	20	0, 20, 40, 60, 80, 100	0	No
3	41–44	20	20, 40, 60, 80	30	No
3	45–48	20	20, 40, 60, 80	70	No
3	49–52	20	20, 40, 60, 80	100	No
4	53–56	20	20, 40, 60, 80	0	Yes
4	57–60	20	20, 40, 60, 80	30	Yes
4	61–64	20	20, 40, 60, 80	70	Yes
4	65–68	20	20, 40, 60, 80	100	Yes

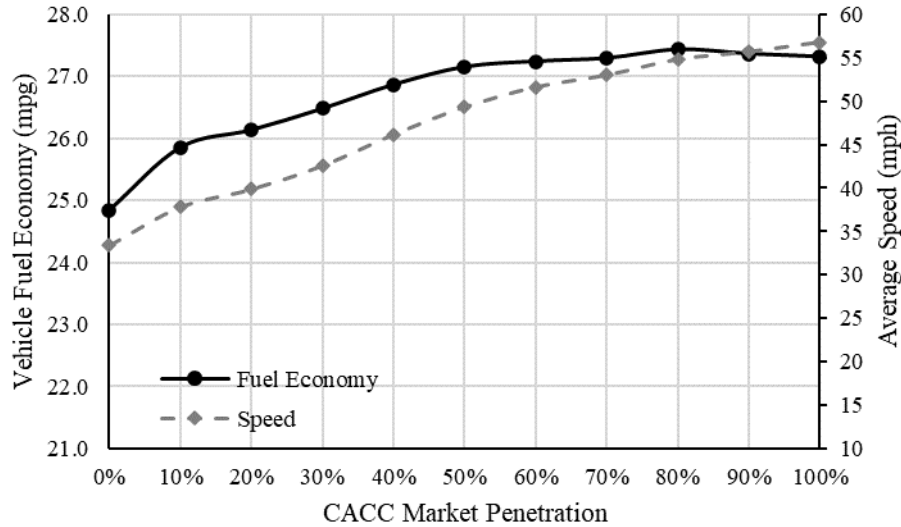
This case study considered 0-, 20-, 40-, 60-, 80-, and 100-percent CACC market penetration rate scenarios. The VAD and ML strategies are only meaningful in mixed traffic conditions. Since there are no manually driven vehicles in the 100-percent CACC scenarios and all vehicles are manually driven in the baseline CACC scenarios, VAD and ML implementation is not considered in those scenarios. The leftmost lane was used as the CACC ML in the studies.

### SIMULATION RESULTS FOR DIFFERENT SCENARIOS

#### CACC Effects at Different Market Penetration Rates

The effects of CACC vehicles on traffic performance and fuel consumption are shown in figure 10. All vehicles, including those in the freeway mainline and on- and off-ramp lanes were counted to calculate these parameters. The free-flow speed is 65 mph for the freeway and 45 mph for the ramps. The speed curve shows that the average vehicle speed increases almost linearly as CACC market penetration increases. At 100-percent CACC market penetration, the average speed is about 56 mph, which is 70 percent higher than the speed at baseline CACC market penetration. The average speed of 56 mph is close to the free-flow speed. This result indicates that equipping all vehicles with CACC nearly eliminates traffic congestion. As traffic

congestion decreases with the increase of CACC market penetration, average vehicle energy fuel economy improves as well. When CACC market penetration is 40 percent or higher, vehicle fuel economy does not increase as rapidly as it does in strategies with lower CACC market penetration rates.

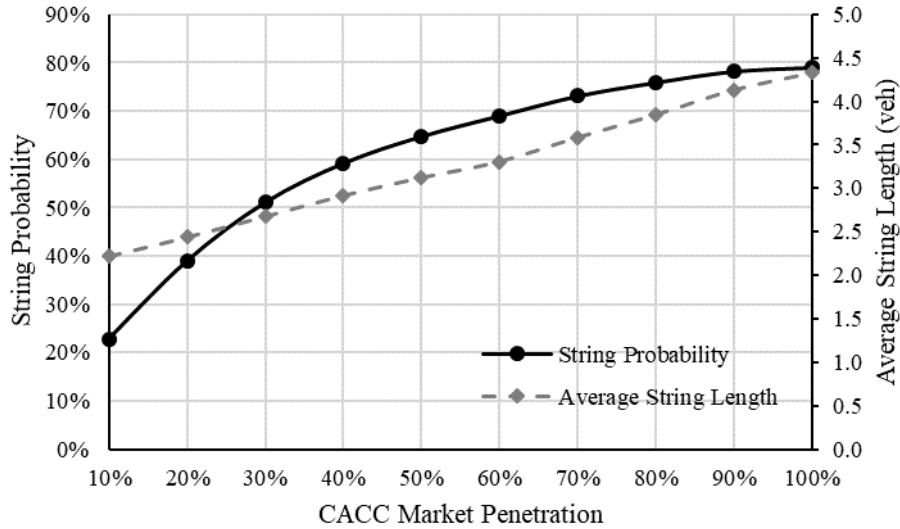


Source: FHWA.

**Figure 10. Graph.  $\bar{v}$  and  $\overline{mpg}$  under various CACC market penetration rates.**

This study examined string operation based on the results shown in figure 11, which indicate string probability increases as CACC market penetration increases. The research team expected this increase because the opportunity for randomly dispersed CACC vehicles to form strings increases as market penetration rates rise. However, the string probability curve becomes flatter as the CACC market penetration rate increases. Even when all vehicles are CACC vehicles, string probability is about 80 percent, indicating the remaining 20 percent of CACC vehicles would not travel in strings. When CACC market penetration is low (e.g., 10 or 20 percent), string probability is higher than the theoretical string probability—which is equal to the CACC market penetration rate. This trend is a result of CACC vehicles’ tendency to stay within the string once they join a string leader. They will not make discretionary lane changes to exit the string even if traffic in the adjacent lanes is moving at a higher speed than the current lane. As a result, more CACC vehicles join strings than leave strings during any given period of time. This tendency results in a string probability higher than the CACC market penetration rate.

The shape of the average string length is different from the shape of the string probability curve. The string length increases linearly with CACC market penetration. In the experiment, the maximum string length is 15 vehicles. However, the average string length is substantially smaller than the maximum string length. In mixed traffic, where manually driven vehicles could cut in or out of the strings, it is difficult for strings to reach the maximum length. In addition, CACC vehicles have different desired speeds. CACC string followers may not be able to catch up with a string leader if it has a higher desired speed. This inability leads to string split, thus reducing average string length.

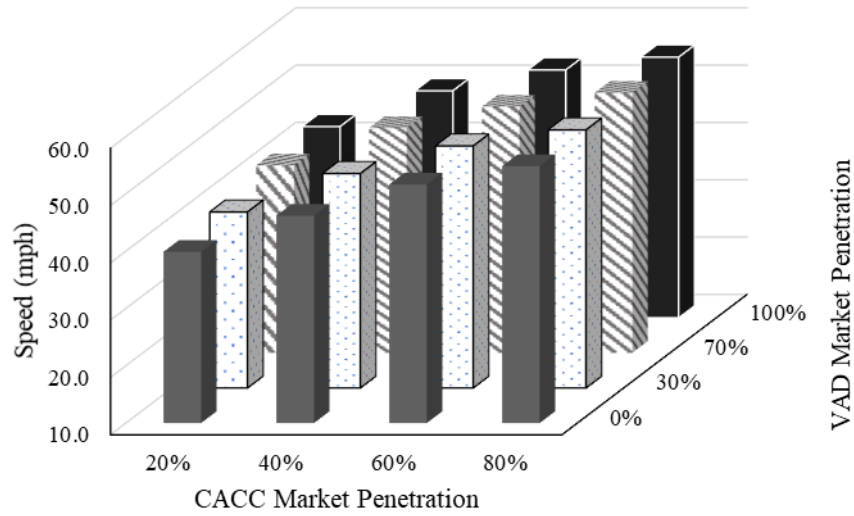


Source: FHWA.  
veh = vehicles.

**Figure 11. Graph.  $P_{string}$  and  $L_{string}$  under various CACC market penetration rates.**

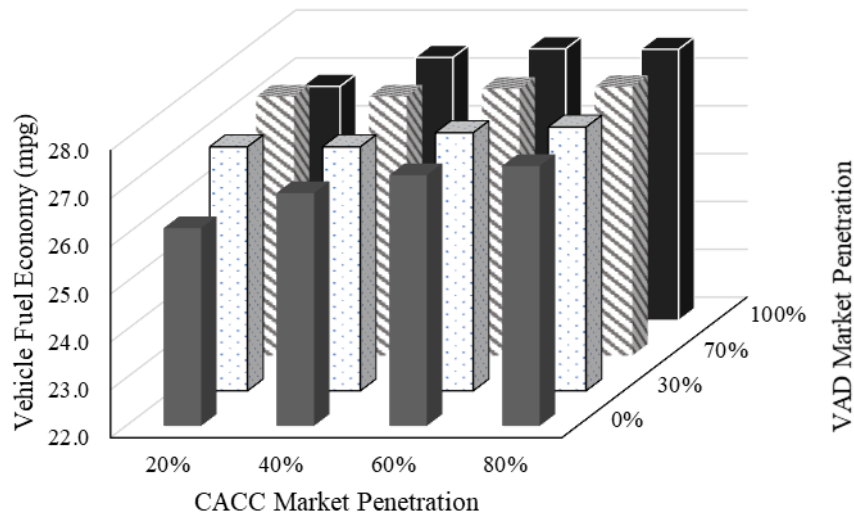
### VAD Effects at Different Market Penetration Rates

Figure 12 and figure 13 show the impacts of VAD on speed and mpg. VAD application significantly affects average vehicle speed when CACC market penetration is 40 percent or lower. In those scenarios, CACC vehicles have difficulty finding string leaders because they are randomly distributed in the traffic stream. Once VAD is deployed, VAD vehicles can be string leaders, enabling isolated CACC vehicles to enter and operate in the string. The increase of CACC strings helps stabilize traffic flow and increase overall speed. When CACC market penetration is greater than 40 percent, CACC vehicles can more easily identify CACC vehicle leaders (i.e., string probability is 70 percent or more, see figure 11). In this strategy, the connectivity capability of VAD vehicles is utilized less, and the influence of VAD strategy on speed therefore decreases. In contrast, VAD strategy minorly influences fuel consumption. When a CACC vehicle follows a VAD vehicle, the CACC controller generates a vehicle trajectory similar to that of the preceding manually driven vehicle. As a result, the energy consumption pattern of CACC vehicles is identical to that of human-driven vehicles. Such car-following behavior does not significantly change fuel consumption patterns of the traffic flow.



Source: FHWA.

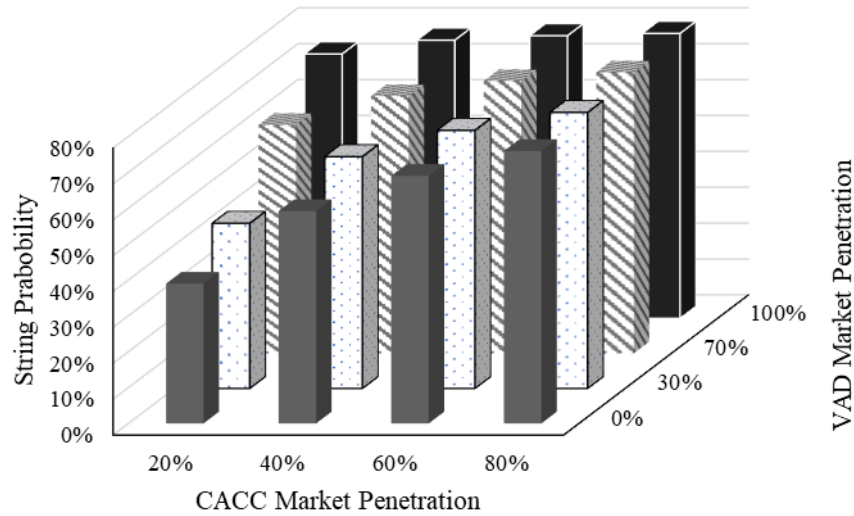
**Figure 12. Chart.  $\bar{v}$  under various VAD market penetration rates.**



Source: FHWA.

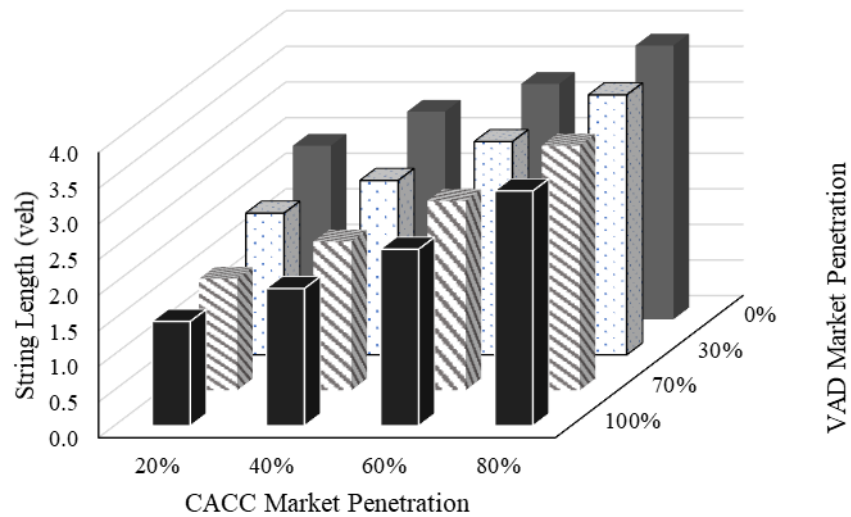
**Figure 13. Chart.  $\overline{mpg}$  under various VAD market penetration rates.**

The VAD strategy significantly influences CACC string operations under low CACC market penetration rate scenarios (figure 14 and figure 15). In figure 15 the VAD axis is reversed for better visualization. At the 20-percent CACC market penetration rate, string probability increases quadratically as VAD market penetration increases, with string probability reaching nearly 80 percent when VAD market penetration is 100 percent. This probability is close to the level of string probability under the 100-percent CACC market penetration rate scenario. In contrast, implementing the strategy results in many short strings containing a VAD leader and one or two CACC followers. This structure causes a decrease in the average string length.



Source: FHWA.

**Figure 14. Chart.  $P_{string}$  under various VAD market penetration rates.**



Source: FHWA.

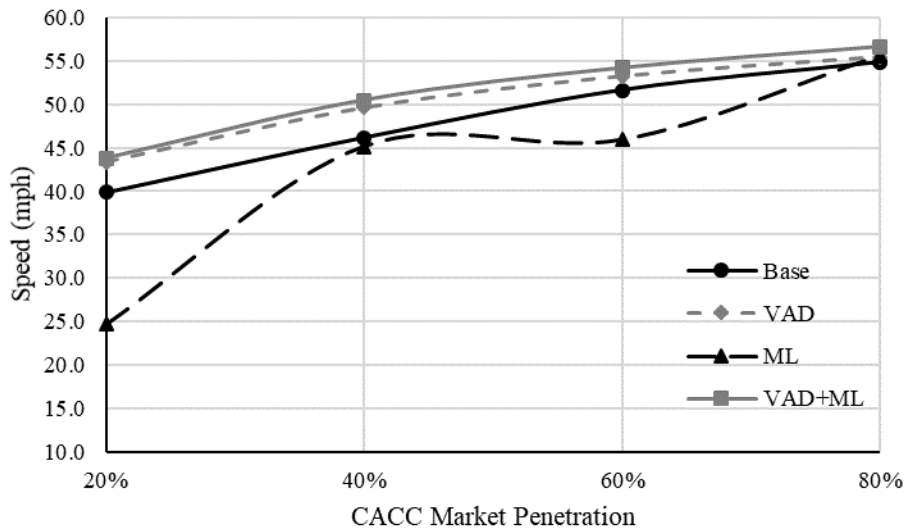
veh = vehicles.

**Figure 15. Chart.  $L_{string}$  under various VAD market penetration rates.**

### Effects of Applying a CAV-Only ML

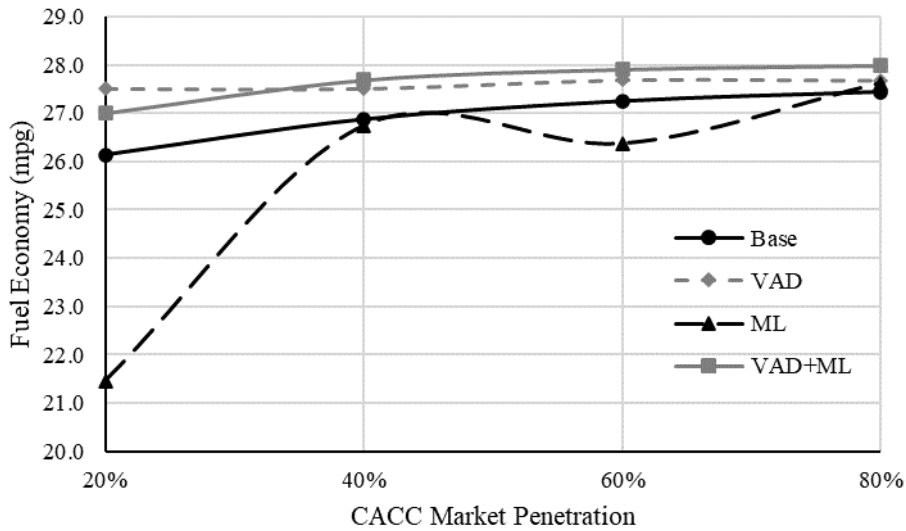
Figure 16 and figure 17 show that the ML strategy alone does not improve either freeway speed or fuel efficiency. When the strategy is implemented, it motivates CACC vehicle drivers to make lane changes toward the ML. These lane changes disturb traffic in the general-purpose lane when the CACC vehicles enter the freeway via on-ramps. In this case, the vehicles need to make three or four consecutive lane changes before they can merge into the ML. Such frequent lane-changing behaviors substantially decrease the stability of the traffic flow. As such, combining the ML and VAD operations decreases the vehicle fuel economy more as compared to the VAD-only scenario. Since this strategy allows more vehicles to operate in CACC mode,

the results indicate that the CACC controller does not produce energy-optimal control commands when the CACC vehicle is in CF.



Source: FHWA.

**Figure 16. Graph.  $\bar{v}$  under the influence of VADs and MLs.**

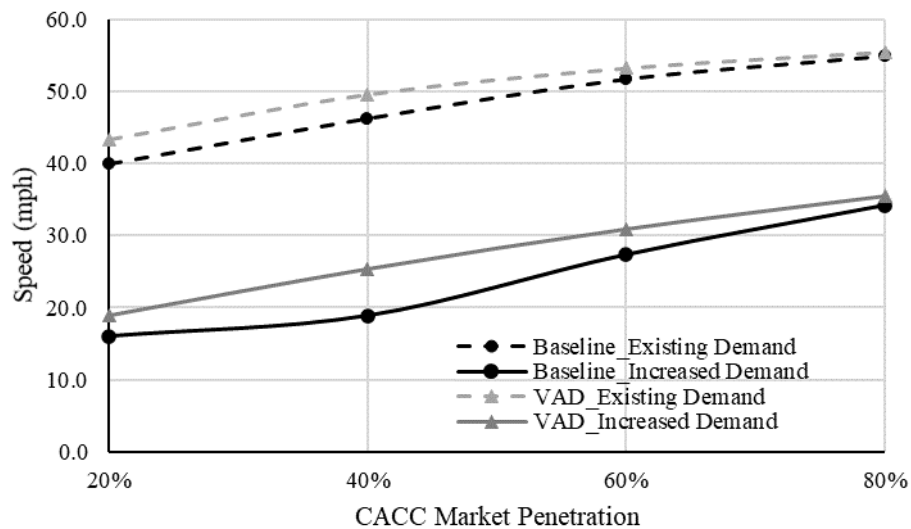


Source: FHWA.

**Figure 17. Graph.  $\overline{mpg}$  under the influence of VADs and MLs.**

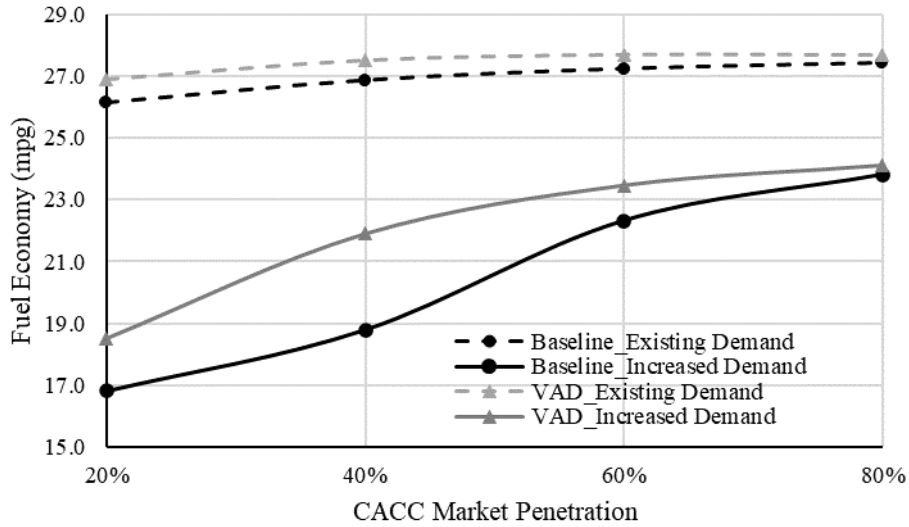
## Effects of Traffic Demand Increase

Previous analysis showed that the ML strategy did not benefit traffic and vehicle energy performance because it disturbed traffic in the general-purpose lanes. With traffic demand increase, the research team expected the negative impact of the ML strategy to increase because the increased demand intensified the congestion level of the corridor. The disturbances caused by the ML strategy further triggered traffic breakdowns under more unstable traffic conditions. For this reason, the ML strategy was not considered in the increased demand strategies. Only the VAD strategy was considered for the increased demand scenarios. Figure 18 and figure 19 show the speed and mpg levels with and without the demand increase. The results indicated that the average speed was greatly affected by the demand increase. The speed decrease was around 22 mph regardless of the CACC market penetration rate, which represented a decreased percentage ranging from 38 to 60 percent. The mpg decrease was not as significant as the speed decrease in the increased demand scenarios. The largest decrease was found under the 20-percent CACC market penetration rate scenario. The mpg dropped from 26.1 to 16.8, which accounted for a 36-percent decrease. Among all the strategies, the mpg decrease ranged from 13 to 24 percent. The results also showed that the effect of the VAD strategy was higher in the demand increase scenarios, which further validated implementing the VAD strategy.



Source: FHWA.

**Figure 18. Graph.  $\bar{v}$  with and without demand increase.**



Source: FHWA.

**Figure 19. Graph.  $\overline{mpg}$  with and without demand increase.**

This study examined the performance of the SR 99 corridor when the traffic demand was increased by 20, 30, and 40 percent. The purpose of the analysis was to identify the amount of extra traffic input the corridor could accommodate with CACC string operation implemented while maintaining the same average speed level observed at the baseline CACC strategy. The results are shown in table 4. In the table, N/A means that the simulation could not be completed within 48 hr because the traffic became so congested that the simulation run could not be handled by a computer with a 6-core processor and 32-GB RAM. When the CACC market penetration rate was 60 percent or lower, the corridor could not handle a 20-percent traffic demand increase while maintaining the baseline average speed. When the CACC market penetration rate was 80 percent, the corridor could serve 120 percent of the current demand. As the CACC market penetration rate reached 100 percent, the demand could be increased by 30 percent.

**Table 4.  $\bar{v}$  (mph) under different traffic demand inputs.**

CACC Market Penetration Rate (%)	100% Demand	120% Demand	130% Demand	140% Demand
0	33.4	N/A	N/A	N/A
20	39.9	16.0	N/A	N/A
40	46.2	18.9	N/A	N/A
60	51.6	27.3	14.0	11.7
80	54.8	34.2	19.2	12.8
100	56.8	45.3	33.4	19.4

N/A = simulation could not be completed within 48 hr.

## RESULTS DISCUSSION

The simulation results show that the traffic performance of the SR 99 corridor increases with CACC market penetration. However, such an improvement is not as significant as the improvement identified at an isolated freeway on-ramp bottleneck.<sup>(1)</sup> At the isolated bottleneck, the freeway pipeline capacity increases by about 90 percent when the CACC market penetration rate rises from baseline to 100 percent. On the SR 99 corridor, the entire network becomes very congested in the 100 percent CACC scenario when the traffic demand increases only by 30 percent. This comparison suggests that it is difficult to extend the same level of CACC benefit observed at individual bottlenecks to larger freeway corridors. One reason for this difficulty is that CACC does not improve bottleneck performance consistently along the corridor. While it significantly affects bottlenecks with smaller disturbances caused by on- and off-ramp traffic, it is less effective at larger bottlenecks where the traffic flow is frequently interrupted by entering and exiting traffic.

In many cases, CACC improved some upstream mild bottlenecks, allowing those bottlenecks to release more vehicles downstream. This trend increased the input flow for downstream heavy bottlenecks. As a result, those heavy bottlenecks became more congested. The traffic congestion at those sites eventually propagated upstream, negatively impacting how upstream bottlenecks were operating. The benefit of CACC was largely offset by the spatial development of the congestion region. This observation indicates the need to develop advanced speed harmonization strategies for the study corridor. The strategy should be able to dynamically adjust the input and output flow of individual bottlenecks by providing CACC vehicles with tailored speed limits. As a result, the strategy can then maintain efficient operation at the busiest bottlenecks using CACC capability while avoiding backward queue propagation. Consequently, this strategy could improve the performance of the entire corridor.

The CACC application positively impacted vehicle fuel efficiency, with the highest average mpg of 27 achieved when the CACC market penetration was higher than 50 percent. This average was 10 percent higher than the baseline strategy. At all CACC market penetration rates of 50 percent or higher, the vehicle fuel efficiency was very similar. CACC string operation significantly improved mpg in the low to medium CACC market penetration scenarios because it mitigated traffic congestion. As the traffic flow became more stable, the overall vehicle energy efficiency improved. When CACC market penetration exceeded 50 percent, the opposing effects of traffic flow smoothing and higher speed balanced each other, leaving net vehicle fuel economy close to constant.

The analysis results show that string probability is 80 percent when all vehicles are equipped with CACC. The remaining 20 percent of vehicles do not operate in strings because they travel as isolated vehicles in the traffic stream. They could be so far from the downstream or upstream strings that they cannot send or receive real-time information to or from the strings. CACC vehicle strings could also be nearby but traveling in different lanes. Those isolated vehicles do not make lane changes to join the strings. In both cases, the vehicles can use a local or regional CACC string-forming algorithm that provide those isolated vehicles with string formulation guidance. Using the algorithm allows the vehicles to plan their trajectories and eventually join the string. Such a string-forming algorithm can help integrate the isolated CACC vehicles into a string, leveraging the overall efficiencies associated with car-following behavior within a string.

Another major case study observation is that the CACC ML strategy does not improve CACC operations. This lack of improvement is a result of CACC vehicles entering from the on-ramps needing to make several lane changes before they can merge into the ML. These lane changes disturb the traffic in general-purpose lanes, leading to degraded traffic operation. Previous studies that implemented the ML strategy at a simple on-ramp bottleneck determined the strategy substantially improved speed and energy on the network.<sup>(1)</sup> This improvement is due to the majority of simulated CACC vehicles having already traveled in the ML when they are released into the simulation network. Those vehicles do not cause lane-changing disturbances to traffic. The study implies that the ML strategy can be used to enhance corridor performance if it is possible to reduce the impact of the lane changes made by CACC vehicles. One potential way to resolve this challenge is to provide dedicated on-ramps for the MLs. Dedicated on-ramps allow CACC vehicles to directly merge into the ML without disrupting the traffic stream in the general-purpose lane. The on-ramps also allow the CACC vehicles to concentrate in the ML, generating efficient traffic flow by forming CACC string operations.

## CHAPTER 6. CONCLUSIONS

### SUMMARY OF STUDY FINDINGS

The purpose of this report is to document a simulation-based case study investigating the effectiveness of SAE Level 1 automation technology for mitigating or solving existing transportation problems related to congestion, fuel consumption, and emissions.<sup>(1)</sup> Specifically, the research team conducted microscopic traffic simulation studies to evaluate how CACC string operation impacts mobility and energy consumption on the SR 99 corridor. The research team analyzed the performance of the 13-mi corridor under various CACC market penetration rates (i.e., 0, 20, 40, 60, 80, and 100 percent), different traffic demands, (i.e., current demand, 120 percent of current demand, 130 percent of current demand, and 140 percent of current demand) and different CACC management strategies (i.e., VADs and CACC and ACC MLs). This study examined average vehicle speed, average mpg, average string length, and CACC vehicle string probability at various CACC market penetration rates. In addition, the research team investigated the spatiotemporal traffic patterns of the corridor under both existing traffic demand and a 20-percent traffic demand increase.

The case study revealed that the average speed of the SR 99 corridor increases linearly with CACC market penetration rates. The average speed increases by 70 percent (e.g., from 34 to 56 mph) at the 100-percent CACC market penetration rate compared to the baseline CACC market penetration rate. The improvement in average speed indicates that CACC string operations substantially improve traffic mobility performance on the corridor.

CACC also impacted fuel efficiency. The analyses show that the average mpg first increased as CACC market penetration increased but started to decrease as the CACC market penetration rate reached 40 percent or higher. The highest average mpg was observed under the 30-percent CACC market penetration rate, at which mpg reached 26, which was 5 percent higher than the baseline strategy. As the CACC market penetration rate reached 100 percent, mpg dropped to 22, which was 11 percent lower than the baseline mpg. CACC string operation improved the mpg at low to medium CACC market penetration rates because it mitigated traffic congestion. As the traffic flow became more stable, overall vehicle energy efficiency increased. When the CACC market penetration rate exceeded 40 percent, traffic flowed at higher speeds, which did not produce optimal vehicle fuel economy. In addition, the study did not consider fuel consumption optimization when designing the acceleration behavior of the CACC controller. This lack of consideration further degraded overall vehicle energy efficiency. A proper energy consumption model will need to be developed to evaluate different levels as they also affect simulation outcome. The research team suggests that energy consumption optimization and reasonably accurate energy consumption models be developed in the future together with CACC controller design improvements to optimize energy consumption for CACC vehicle operation.

The corridor allowed about 30 percent more traffic to enter the network without experiencing reduced travel time at the 100-percent CACC market penetration rate. This rate was much lower than the capacity increase (i.e., 90 percent) identified at a simple on-ramp bottleneck. Performance improvement at an isolated bottleneck increased the output flow to the downstream segments on the freeway corridor, which led to reduced mobility for downstream bottlenecks. As

such, reducing congestion at isolated bottlenecks did not necessarily bring about a benefit of the same magnitude for the entire corridor. This observation indicates the need for developing corridor-level traffic flow–management strategies (e.g., variable speed limit (VSL) signs and variable speed advisories (VSAs) including speed harmonization) to coordinate the input and output flow of each bottleneck to maximize overall throughput. Such strategies could enhance the effectiveness of CACC for complicated freeway systems.

The analysis results showed that CACC string probability was 80 percent even when all vehicles were equipped with CACC. The remaining 20 percent of vehicles did not operate in strings because they were far from the upstream or downstream strings or they could not identify the strings in adjacent lanes. If CACC string probability approached 100 percent (i.e., if all CACC vehicles joined strings), traffic flow would further improve. This trend suggests the need to develop local or systematic string-forming strategies to help isolated CACC vehicles. String performance should substantially increase once the current ad hoc string scheme is replaced by those strategies, leading to improved traffic throughput.

VAD and CACC ML strategies were also considered in the case study. The VAD strategy enhanced CACC string operation by increasing string probability since it allowed VAD vehicles to behave like CACC string leaders without compromising performance. Increasing the number of manually driven vehicles equipped with VAD allowed CACC vehicles to locate string leaders more easily. This strategy had the greatest influence at CACC market penetration rates between 20 and 40 percent. In those scenarios, the average speed increased by 8 percent, while mpg remained similar. When the CACC market penetration rate increased above 40 percent, CACC vehicles located CACC string leaders more easily, which reduced the effectiveness of the VAD strategy. For example, both the speed and mpg fuel consumption variations under 80-percent CACC market penetration scenarios were only about 1 percent.

In contrast, the ML strategy decreased corridor performance when it was implemented alone. This decrease was a result of the strategy encouraging CACC vehicles to merge into the ML. These lane-changing maneuvers disturbed the general-purpose lanes, making the traffic flow in those lanes unstable. The research team determined dedicated on-ramps that allow CACC vehicles to enter the ML directly will address this challenge.

## **SUMMARY OF IMPACTS**

The opportunity to improve traffic operations expands as the number of CAVs on freeways increases. Results from this simulation study show that the use of CACC on SR 99 could significantly improve travel time and smooth the flow of traffic. Effective use of CACC on SR 99 and other California freeways could be a potential strategy for continued improvement of our transportation system.

Caltrans has funded several past and ongoing projects on advanced technologies for active traffic management (ATM), including the following:

- CRM field operational test on an SR 99 northbound section near Sacramento (2015–2017).<sup>(18)</sup>
- VSA field operational test on SR 78 eastbound between Vista Village Drive (in the city of Vista) and the freeway interchange point of SR 78 East and U.S. Route 15 (in the city of Escondido) (2016–2018).<sup>(19)</sup>
- Coordination of freeway ramp metering and arterial traffic signal control—field operational test (2013–2019), Phase I: one on-ramp and one intersection in San Jose: SR 87 and Taylor Street; Phase II: I-680 and Capitol Avenue in San Jose, involving a freeway corridor of five on-ramps and multiple intersections.<sup>(20)</sup>
- Combined VSA and CRM field operation test on SR 99 northbound between Elk Grove Boulevard and SR 50 interchange (ongoing project).<sup>(21,22)</sup>

CVs and CAVs have the potential to be used as sensors for better traffic detection. CAVs also have the potential to act as control actuators for VSA because the advisory speed determined by the TMC could be passed to the CAV and used as the set speed to regulate traffic. The same concept could be used to control intersection traffic signals.

Caltrans continues to support the use of advanced technology to improve ATM system capabilities on its freeways. This case study has shown that integrating CAV technology into ATM strategies can improve both the efficiency and the effectiveness of these strategies. Caltrans continues to explore incorporating CACC and other CAV concepts into its future ATM strategies.

## **LIMITATIONS OF THE STUDY AND SUGGESTIONS FOR ADDITIONAL RESEARCH**

This study only considered CACC vehicle string operation for passenger vehicles. However, the truck platooning operation is expected to be progressively adopted by the freight industry in the next few years. When passenger vehicles share the road with long truck strings, their lane-changing and car-following patterns may be very different from current behaviors. In addition, the string-forming and string-splitting strategies and algorithms for handling cut-ins and cut-outs might need to be revisited as these trucks start joining CACC vehicle strings. These considerations should be included in future investigations.

The case study also identified several challenges of implementing CACC and CACC management strategies on the study corridor. These challenges can be addressed by deploying advanced traffic flow-management algorithms (e.g., VSL and VSA), implementing local or regional CACC string-forming strategies, adding new infrastructure (e.g., dedicated on-ramps) to the existing freeway system, or any combination of the three. For example, implementing VSLs and VSAs that send tailored speed limit or advisory messages to individual CAVs via vehicle-to-infrastructure (V2I) communications can help smooth traffic flow on the corridor,

leading to high vehicle throughput without traffic breakdowns. Another potentially helpful CAV application coordinates vehicle merge maneuvers by sending recommended trajectories to the merging vehicles and vehicles traveling in the target lane. This merge coordination application can reduce disturbances caused by on-ramp traffic, potentially diminishing the congestion at on-ramp bottlenecks. To study the impacts of the CACC string formation, VSLs/VSAs, and trajectory control, it will be necessary to develop control algorithms and add V2I modeling capabilities into the existing traffic simulation framework. Such analyses are left for future research.

## REFERENCES

1. SAE J3016. (2018). *Taxonomy and Definitions for Terms Related to Driving Automation Systems for On-Road Motor Vehicles*, SAE International, Warrendale, PA. Available online: [https://www.sae.org/standards/content/j3016\\_201806](https://www.sae.org/standards/content/j3016_201806), last accessed September 29, 2020.
2. Liu, H., Kan, X., Shladover, S.E., Lu, X.-Y., and Ferlis, R.E. (2018). “Impact of Cooperative Adaptive Cruise Control on Multilane Freeway Merge Capacity.” *Journal of Intelligent Transportation Systems*, 22(3), pp. 263–275, Institute of Electrical and Electronics Engineers, Piscataway, NJ.
3. Larson, J., Kammer, C., Liang, K.Y., and Johansson, K.H. (2013). “Coordinated Route Optimization for Heavy-Duty Vehicle Platoons.” Presented at the 16th International IEEE Conference on Intelligent Transportation Systems, The Hague, Netherlands.
4. Larson, J., Liang, K.Y., and Johansson, K.H. (2015). “A Distributed Framework for Coordinated Heavy-Duty Vehicle Platooning.” *IEEE Transactions on Intelligent Transportation Systems*, 16(1), pp. 419–429, Institute of Electrical and Electronics Engineers, Piscataway, NJ.
5. Liang, K.Y., Mårtensson, J., and Johansson, K.H. (2013). “When Is It Fuel Efficient for a Heavy Duty Vehicle to Catch Up With a Platoon?” *IFAC Proceedings Volumes*, 46(21), pp. 738–743, Elsevier, Amsterdam, Netherlands.
6. Shladover, S.E., Su, D., and Lu, X.-Y. (2012). “Impacts of Cooperative Adaptive Cruise Control on Freeway Traffic Flow.” *Transportation Research Record: Journal of the Transportation Research Board*, 2324, pp. 63–70, Transportation Research Board, Washington, DC.
7. Lu, X.-Y., Chen, D., and Shladover, S.E. (2014). Preparations for Field Testing of Combined Variable Speed Advisory (VSA) and Coordinated Ramp Metering (CRM) for Freeway Traffic Control, Report No. CA14-2292, California Department of Transportation, Sacramento, CA.
8. Caltrans. (2020). “Caltrans Performance Measurement System (PeMS).” (website). Available online at <http://pems.dot.ca.gov>, last accessed April 28, 2020.
9. Yeo, H., Skabardonis, A., Halkias, J., Colyar, J., and Alexiadis, V. (2008). “Oversaturated Freeway Flow Algorithm for Use in Next Generation Simulation.” *Transportation Research Record: Journal of the Transportation Research Board*, 2088, pp. 68–79, Transportation Research Board, Washington DC.
10. Milanés, V. and Shladover, S.E. (2014). “Modeling Cooperative and Autonomous Adaptive Cruise Control Dynamic Responses Using Experimental Data.” *Transportation Research Part C: Emerging Technologies*, 48, pp. 285–300, Elsevier, Amsterdam, Netherlands.

11. Milanés, V., Shladover, S.E., Spring, J., Nowakowski, C., Kawazoe, H., and Nakamura, K. (2014). “Cooperative Adaptive Cruise Control in Real Traffic Situations.” *IEEE Transactions on Intelligent Transportation Systems*, 15(1), pp. 296–305, Institute of Electrical and Electronics Engineers, Piscataway, NJ.
12. Lu, X.-Y., Kan, X.D., Shladover, S.E., Wei, D., and Ferlis, R.A. (2017). “An Enhanced Microscopic Traffic Simulation Model for Application to Connected Automated Vehicles.” Presented at the Transportation Research Board 96th Annual Meeting, Washington, DC.
13. Xiao, L., Wang, M., and van Arem, B. (2017). “Realistic Car-Following Models for Microscopic Simulation of Adaptive and Cooperative Adaptive Cruise Control Vehicles.” *Transportation Research Record: Journal of the Transportation Research Board*, 2623, pp. 1–9, Transportation Research Board, Washington, DC.
14. Liu, H., Kan, X.D., Shladover, S.E., Lu, X.-Y., and Ferlis, R.E. (2018). “Modeling Impacts of Cooperative Adaptive Cruise Control on Mixed Traffic Flow in Multi-Lane Freeway Facilities.” *Transportation Research Part C: Emerging Technologies*, 95, pp. 261–279, Elsevier, Amsterdam, Netherlands.
15. Aimsun. (2020). “Aimsun Next Tech Specs.” (website). Available online at <https://www.aimsun.com/about-aimsun>, last accessed on October 6, 2020.
16. Rakha, H., Ahn, K., Moran, K., Saerens, B., and Van den Bulck, E. (2011). “Virginia Tech Comprehensive Power-Based Fuel Consumption Model: Model Development and Testing.” *Transportation Research Part D: Transport and Environment*, 16(7), pp. 492–503, Elsevier, Amsterdam, Netherlands.
17. Department for Transport. (2018). *Transport Analysis Guidance, The Transport Appraisal Process*, Department for Transport, London, UK.
18. Lu, X.-Y., Amini, Z., Mauch, M., and Skabardonis, A. (2019). *Congestion-Responsive On-Ramp Metering: Recommendations toward a Statewide Policy*, Report No. UCB-ITS-PRR-2019-01, California Partners for Advanced Transportation Technology, Richmond, CA.
19. Lu, X.-Y., Spring, J., Wu, C.J., Nelson, D., and Kan, Y.H. (2019). *Field Experiment of Variable Speed Advisory (VSA), Final Report*, Report No. UCB-ITS-PRR-02, 2019, California Partners for Advanced Transportation Technology, Richmond, CA.
20. Lu, X.-Y., Wu, C.J., Spring, J., and Shladover, S.E. (2017). *Field Test of Coordinated Ramp Metering*, Report No. UCB-ITS-PRR-2017-01, California Partners for Advanced Transportation Technology, Richmond, CA.
21. Kan, D., Lu, X.-Y., and Skabardonis, A. (2016). *Coordination of Freeway Ramp Meters and Arterial Traffic Signals – Site Selection and Simulation Development*, Report No. UCB-ITS-PRR-2016-06, California Partners for Advanced Transportation Technology, Richmond, CA.

22. Lu, X.-Y., Su, D.Y., and Spring, J. (2014). *Coordination of Freeway Ramp Meters and Arterial Traffic Signals Field Operational Test (FOT), Final Report*, Report No. UCB-ITS-PRR-2014-2, California Partners for Advanced Transportation Technology, Richmond, CA.





